Compensating for Stimulated Echoes in Quantitative T2 Relaxometry

Dushyant Kumar[1,2], Susanne Siemonsen[1,3], Jens Fiehler[1], and Jan Sedlacik[1]

[1]*Neuroradiology, Universitätsklinikum Hamburg-Eppendorf, Hamburg, Hamburg, Germany,* [2]*Multiple Sclerosis Imaging Section (SeMSI), Universitätsklinikum Hamburg-Eppendorf, Hamburg, Germany, Germany,* [3]*Multiple Sclerosis Imaging Section (SeMSI), Universitätsklinikum Hamburg-Eppendorf, Hamburg, Hamburg, Germany*

Target Audience: Researchers interested in quantitative T2 relaxometry (QT2R)

INTRODUCTION: The QT2R has been successfully used to monitor tissue damages in demyelinating neurological disease such as multiple sclerosis(1), stroke and other diseases. However, the voxelwise T2-decay deviate significantly from multi-exponential (ME) model due to the stimulated emission (SE) resulting from the imperfect slice profile of refocusing pulses and the B1-error and so, following ME model would lead to serious quantification inaccuracy. A novel post-processing method to compensate for B1 error is being presented using only QT2R data. The slice profile or refocusing pulse was optimized by choosing the slice thickness of refocusing pules to be 3 times that of excitation pulse (2).

THEORY: For known B1-error (flip angle error) and the T2 distribution, the T2-decay is given by extended phase graph (EPG) model (4). However, this model can be linearized and can be given by: $y = A^{EPG}x + \varepsilon$, with $A^{EPG}(i,j)$ = intensity at echo time-point TE(i) due to unit volume fraction at with discrete T2 value T2(j). To make the reconstruction more noise robust, the prior expectations regarding the spatial smoothness is implemented as described in (3): $\hat{\mathbf{x}}=\arg\min_x \left\|\mathbf{A}_{ex}\bar{\mathbf{x}}-\bar{\mathbf{y}}\right\|^2+M_T\left\|\bar{\mathbf{x}}\right\|^2+\mu_S\left\|\mathbf{D}_S\bar{\mathbf{x}}\right\|^2;\mathbf{x}\geq 0$ [1], where the single-voxel quantities **x, y, ε** are collected into multi-voxel column vectors and $\mathbf{A}_{ex}$ is the block diagonal matrix, with A^{EPG} as its block. M_T is the diagonal matrix with voxelwise temporal regularization μ_T along its diagonal and μ_S is spatial regularization parameter. Matrix D_S is first difference operator, the norm $||D_S\,\bar{\mathbf{x}}||$ penalizes non-smooth solutions for each T2-points.

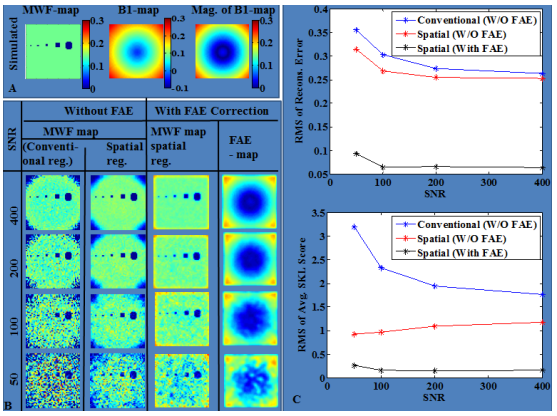

Fig 1: (A) Simulated MWF map and B1 map along with its absolute map (B) Reconstructions (MWF-maps and FAE-maps) at various SNR using both methods: with and without FAE correction. (C) Relative mean square of reconstructed MWF maps and averaged SKL scores as a function of SNRs for three different reconstruction approaches.

DATA AND METHODS: *Experiment:* The QT2R data was acquired from phantom (1 liter H_20 with 1.25 g NiSO4 + 5 g NaCl) and healthy volunteers using 2D CPMG sequence (3T Siemens Skyra) with: axial FOV 240 mm, matrix size 128x96, receiver bandwidth 355 kHz, 8 slices, slice thickness 4 mm, TR 2000 ms, 32 echoes, PAT-factor 2; echo spacing 8.3 ms, acquisition time 22 min. *Simulation:* A numerical phantom consisting of lesions (single pool with T2 of 100 ms) with varying sizes (1-8 voxels) surrounded by matrix (two pools with geometric means T2 of 30 ms and 100 ms) was used.

Processing Algorithm: **(Step 1):** The flip angle errors (FAE) δ_{kl}, along with temporal regularization constant μ_T, are allowed to vary voxelwise. It's effect on excitation and refocusing pulses are assumed to be identical and can be accounted for by a multiplicative factor of $(1+\delta_{kl})$ for $(k,l)^{th}$ voxel. Using the EPG model for MESE sequence (flip angles 90^0, 180^0), only the magnitude of the FAE could be detected and not its sign. 60 possible candidates for δ_{kl}'s are selected between 0 % to 30% at regular intervals. This step is equivalent to setting $\mu_S = 0$ in eqn [1] and the suitable value of (μ_T, δ_{kl}) are chosen in two sub-steps: **(Step1-i)** One L-curve (5) is generated for each possible value of δ_{kl}, where data fidelity terms and L2-norm of the solutions are plotted on two axes, with each plot point corresponding to a particular value of μ_T. The elbow of the L-curve is a good compromise between data fidelity and prior at that value of FAE. This is similar to the L-curve approach described by Kumar et al (3), where only even echoes were considered with no FAE correction. **(Step-1-ii)** Corresponding to all possible values of δ_{kl}'s, we would have that many L-curves and that many elbows. These elbow-values are again re-plotted as L-curve and the elbow is again chosen as the best compromise and corresponds to particular values of (μ_T, δ_{kl}). (**Step 2**): Using the δ_{kl} maps or flip angle error (FAE) map derived in the previous step, matrices $\mathbf{A_{ex}}$ is constructed using the EPG model. The spatial regularization constant is chosen as μ_S = 1000*median(μ_T-map). With known FAE-map, M_T and μ_S, eqn [1] can be written as expression with single L2-norm and is solved by sparse nonnegative least square (SNNLS) solver (6) as described in (3). Since the entire slice cannot be processed in one go due to prohibitive slower speed of SNNLS for larger data size, 10 x 10 data selecting window (DSW) was processed and there was overlap between successive DSWs(3).

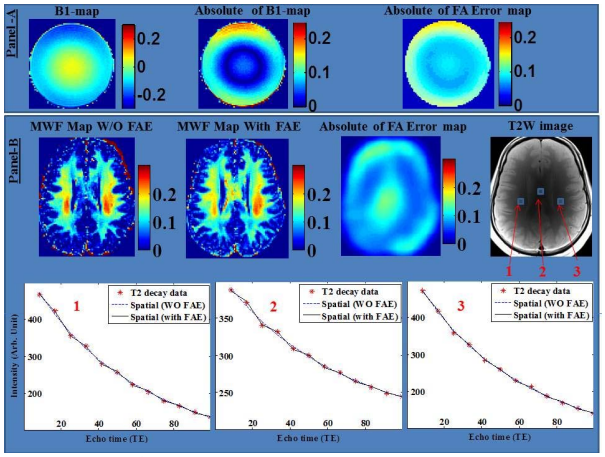

Fig 2: ***Panel-A****: Comparison of B1-map and its absolute are compared against FA error map using the water phantom scan. Panel-B: top row: MWF-map-with-FAE correction method is more consistent with corresponding T2W map in central and outer regions; while disregard for FAE correction results in underestimation of myelin in those part.* ***Panel-B:*** *bottom row: Individual fitted curves using both methods are plotted along with experimental data (only 12 echoes shown for better visualization) for voxels from three regions of interests shown on T2W image in the top row. The spatial-with-FAE correction approach shows better fits in all three voxels.*

RESULTS: *Simulation:* Fig. 1-A depicts simulated myelin and B1 maps; while fig 1-B depicts the simulated and reconstructed MWF maps at various SNRs with and without FAE correction methods. In comparison to the conventional approach, the FAE correction method is better matched to simulated maps with reduced mean square errors (MSE) and lower symmetric Kullbeck-Leibler (SKL) scores for both surrounding matrix and simulated lesions at all SNRs. *Experiment:* (Comparison of B1-map with FAE-map): The B1-map was extracted using two flip angle method. The FAE map, extracted from liquid phantom QT2R data, showed good consistency with absolute value of B1-map. (*Human Scanner):* Figure 2-B; 1st row depicts MWF reconstructions using the spatial-with-FAE-correction approach (SWFC) against spatial-w/o-FAE-correction (SWOFC). In central region, the MWF reconstruction using the SWFC approach is more consistent with our expectation based on the corresponding T2W image; while the other approach underestimates MWF in that area. (*Demonstrating Voxelwise Improvement):* We chose three voxels from three ROIs as shown on the T2W image in Fig 2-B; 2nd row. As can be seen, the SWFC approach gives better fit to the experimental data for all three ROIs.

DISCUSSION: Our preliminary results show that rather than discarding the odd echoes of CPMG based QT2R analysis, the noise robustness of reconstruction can be improved by incorporating all echoes along with flip angle error correction method described here. Also, our approach is consistent with most popular multi-exponential-nonnegative-least-square framework (1,3).

CONCLUSION: A significant improvement in myelin quantification is demonstrated in areas where flip angle errors are significant (≥8-10%).

References: 1) Laule et al, Mult. Scler. 12(6), 2006; 2) Pell et al, J. of Mag. Res. Imag.;23(2), 2006; 3) Kumar et al, Mag. Res. in Med., 68(5), 2012; 4)Hennig et. al. Mag. Res. in Med, 51(1), 2004; 5) Hansen P.C. ,SIAM Review, 34(4), 1992; 6) Portugal et al, Math. Of Comp., 208, 1994